

GSH depletion, protein S-glutathionylation and mitochondrial transmembrane potential hyperpolarization are early events in initiation of cell death induced by a mixture of isothiazolinones in HL60 cells

Anna Di Stefano ^{a,*}, Simona Frosali ^b, Alessandra Leonini ^a, Anna Ettore ^a, Raffaella Priora ^b,
Francesca Cherubini Di Simplicio ^c, Paolo Di Simplicio ^b

^a Department of Molecular Biology, University of Siena, via Fiorentina 1, 53100 Siena, Italy

^b Department of Neuroscience, University of Siena, via A. Moro, S. Miniato, 53100 Siena, Italy

^c Department of Clinical Medicine and Immunological Sciences, Dermatology Section, University of Siena, Policlinico Le Scotte, viale Bracci, 53100 Siena, Italy

Received 25 August 2005; received in revised form 20 December 2005; accepted 21 December 2005

Available online 18 January 2006

Abstract

We recently described that brief exposure of HL60 cells to a mixture of 5-chloro-2-methyl-4-isothiazolin-3-one (CMI) and 2-methyl-4-isothiazolin-3-one (MI) induces apoptosis at low concentrations (0.001–0.01%) and necrosis at higher concentrations (0.05–0.1%). In this study, we show that glutathione (GSH) depletion, reactive oxygen species generation, hyperpolarization of mitochondrial transmembrane potential ($\Delta \Psi_m$) and formation of protein–GSH mixed disulphides (S-glutathionylation) are early molecular events that precede the induction of cell death by CMI/MI. When the cells exhibit common signs of apoptosis, they show activation of caspase-9, reduction of $\Delta \Psi_m$ and, more importantly, decreased protein S-glutathionylation. In contrast, necrosis is associated with severe mitochondrial damage and maximal protein S-glutathionylation. CMI/MI-induced cytotoxicity is also accompanied by decreased activity of GSH-related enzymes. Pre-incubation with L-buthionine-(S,R)-sulfoximine (BSO) clearly switches the mode of cell death from apoptosis to necrosis at 0.01% CMI/MI. Collectively, these results demonstrate that CMI/MI alters the redox status of HL60 cells, and the extent and kinetics of GSH depletion and S-glutathionylation appear to determine whether cells undergo apoptosis or necrosis. We hypothesize that S-glutathionylation of certain thiol groups accompanied by GSH depletion plays a critical role in the molecular mechanism of CMI/MI cytotoxicity.

© 2006 Elsevier B.V. All rights reserved.

Keywords: Apoptosis; Mitochondrial transmembrane potential; Caspases; Reactive oxygen species; S-glutathionylation; Glutathione

1. Introduction

Cell death occurs by two important mechanisms, apoptosis and necrosis. Induction of the one or the other mechanism depends of the intensity of certain stimuli. Although apoptosis is a protective device for the organism, any deregulation or inappropriate induction of it may cause cell damage and disease [1].

Various agents, including withdrawal of growth factors, oxidative stress, cytokines and anticancer drugs, treatment with

chemicals, DNA-damage inducers and viral infection, can evoke the apoptotic or necrotic programme in a dose-dependent manner [2–9]. Although many studies have established that some early biochemical events are important for the development of apoptosis or necrosis, their reciprocal relationships are still unclear. Similarly, it is unknown how different noxious agents bypass the defence systems to produce cell death. For example, oxidative stress has a well-recognized role in the onset of apoptosis [10,11], but it remains unclear how small doses of oxidants, usually sufficient to trigger the apoptotic machinery, are able to escape from the antioxidant control exerted by GSH and other antioxidants.

We have shown that four preservatives belonging to different chemical classes, namely phenoxyethanol, a mixture of

* Corresponding author. Tel.: +39 0577 234906; fax: +39 0577 234903.

E-mail address: distefano@unisi.it (A. Di Stefano).

chloromethylisothiazolinone (CMI) and methylisothiazolinone (MI), imidazolidinyl-urea and pentanediol, can induce apoptosis vs. necrosis in HL60 cells in vitro [9]. The mixture of isothiazolinones (CMI/MI) was the most toxic of the four preservatives in these cells. Moreover, using independent biochemical indexes of apoptosis, we demonstrated that CMI/MI at low concentrations (0.001% and 0.01%) induces apoptotic cell death at the time interval of 3–6 h (as documented by subdiploid DNA content and phosphatidylserine exposure) via caspase-3 activation. In contrast the HL60 response at higher CMI/MI concentrations (0.05% and 0.1%) was necrosis.

More recently, we confirmed in normal human keratinocytes that apoptosis and necrosis are related to the dose of CMI/MI, and we reported that reactive oxygen species (ROS) generation is an early and causal step in the apoptotic response [12]. We also reported that pre-incubation of keratinocytes with the antioxidant N-acetylcysteine (NAC) completely prevents the appearance of all markers of apoptosis.

Recently, it was reported that the toxic effects of methylisothiazolinone on neurons are mediated by a caspase-independent pathway [13].

Since it has been reported that CMI/MI can interact with glutathione and with sulphhydryl groups of enzymes and other proteins [14–16], we speculate that the reaction of CMI/MI with GSH or specific thiols within cells can perturb the normal redox balance and shift HL60 cells into a state of oxidative stress, which induces apoptosis or necrosis. Recent evidence suggests that the depletion of cellular glutathione, induced by several agents such as phenethyl isothiocyanate, is a stimulus leading to apoptosis in different cell types [17,18]; in particular, a decrease of GSH is closely related to apoptosis in lymphoid cells [19]. In addition, CD95 (FAS/APO-1)-mediated apoptosis was reported to be associated with the rapid loss by efflux of reduced glutathione from cells [20]. In contrast, other authors have suggested that GSH loss alone does not necessarily commit cells to apoptosis [21,22]. If this is true, it remains to clarify which molecular event elicited by ROS is important to induce apoptosis.

In the present study, we used HL60 cells to investigate the role of intracellular thiols in the induction of apoptosis vs. necrosis after CMI/MI treatment; this cell line is very sensitive to various stimuli, including oxidative stress and CMI/MI [9], and is the one most commonly used in the study of apoptosis. HL60 cells were exposed to both apoptotic and necrotic doses of CMI/MI. Using time-course and dose–response experiments (time range: 0–3 h; dose range: 0.001–0.1% CMI/MI), we evaluated the production of reactive oxygen species (ROS), changes in mitochondrial transmembrane potential ($\Delta\psi$ m), and the levels of GSH and cysteine reduced, oxidized and bound to proteins by mixed disulphides.

Our results show that CMI/MI treatment alters the redox state of HL60 cells, the extent and kinetics of which determine the choice between the apoptotic and necrotic modes of cell death. Flow cytometric and HPLC data show that CMI/MI cytotoxicity is associated in a dose-dependent manner with GSH depletion, ROS generation, altered mitochondrial function, and formation of protein–GSH

mixed disulphides, a process known as S-glutathionylation. We hypothesize that S-glutathionylation, in addition to GSH depletion, plays a critical role in the molecular mechanism of CMI/MI toxicity.

2. Materials and methods

2.1. Reagents

A mixture of 5-chloro-2-methyl-4-isothiazolin-3-one and 2-methyl-4-isothiazolin-3-one, in an approximate ratio of 3:1 (CMI/MI, commercially named Kathon CG™, was obtained from Rohm and Haas (Spring House, PA, USA). Foetal calf serum (FCS) was obtained from Gibco (Milan, Italy), Ac-LEHD-pNA from BioSource International distributed in Italy by Prodotti Gianni (Milan, Italy). HPLC-grade reagents were purchased from Mallinckrodt Baker Inc. (Phillipsburg, NJ, USA). The OmniSpher C18 reversed-phase HPLC column (250×4 mm) was purchased from Varian (Lake Forest, CA, USA). Monobromobimane (mBrB) was obtained from Calbiochem (La Jolla, CA, USA). RPMI medium, 2',7'-dichlorofluorescein diacetate (DCFH-DA), *o*-phthalaldehyde (OPT), Rhodamine 123 (Rhod123), propidium iodide (PI), L-buthionine-(S,R)-sulfoximine (BSO), glutathione (GSH), oxidized glutathione (GSSG), N-ethylmaleimide (NEM), dithiothreitol (DTT) and trichloroacetic acid (TCA) were obtained from Sigma-Aldrich Corp. (St. Louis, MO, USA). Fluorescein isothiocyanate (FITC)-labeled AnnexinV (AnnxV) kit was obtained from Boehringer Ingelheim Bioproducts (Vienna, Austria).

2.2. Cell treatment

HL60 cells were donated by Prof. Marcella Cintorino, Policlinico Le Scotte, Siena. The cells were grown in RPMI medium supplemented with 10% foetal calf serum (FCS), glutamine (2 mM), penicillin (100 IU/ml) and streptomycin (100 µg/ml) at 37 °C in a humidified atmosphere containing 5% CO₂.

HL60 cells between the 5th and 20th passage were treated as previously reported [9]. The cells, at the concentration of 5×10^5 /ml, were incubated at 37 °C in RPMI medium containing 10% FCS. After 1 h of incubation, the cells were exposed to increasing concentrations of CMI/MI (0.001–0.1%) for 10 min. They were then washed with phosphate-buffered saline (PBS), collected by centrifugation, resuspended in fresh medium at 1×10^6 cells/ml (0 time) and incubated at 37 °C for different times (1 h and 3 h). At specified times, cells were washed and resuspended in PBS and prepared for specific assays as reported below. Cells treated with vehicle only (PBS) served as controls.

We chose the concentrations 0.001%, 0.01%, 0.05% and 0.1% of CMI/MI solution as supplied by the manufacturer (respectively 0.15, 1.5, 7.5 and 15 ppm of active ingredients). In fact the maximum allowed concentration in “rinse off” products is 0.1% of Kathon CG (sold as a dilute aqueous solution of 1.5% of the two isothiazolinones, corresponding to 15 ppm of active ingredients), while in “leave on” products it is 0.05% (corresponding to circa 7.5 ppm). For GSH depletion, the cells were incubated for 24 h with 500 µM L-buthionine-(S,R)-sulfoximine (BSO) and then treated with CMI/MI as reported above.

2.3. Flow cytometric analysis

2.3.1. Evaluation of ROS production

The formation of intracellular ROS was measured using 2',7'-dichlorofluorescein diacetate (DCFH-DA). By this method, it is possible to measure the amount of H₂O₂ generated by increased oxidative metabolism. Viable cells can deacetylate DCFH-DA to 2',7'-dichlorofluorescein, which is not fluorescent but can react quantitatively with oxygen species within the cell to produce 2',7'-dichlorofluorescein (DCF), which is fluorescent and is trapped inside the cell. The cytofluorimetric measurement of the DCF produced can provide an index of intracellular oxidation [23]. The cells were incubated for 30 min at 37 °C with DCFH-DA (10 µM final concentration). After incubation, the cells were washed with PBS, resuspended in fresh medium and treated with different

concentrations of CMI/MI (0.001–0.1%). For measurement of the intensity of DCF fluorescence, the cells were kept in ice until analysis with a FACSCalibur flow cytometer (Becton Dickinson, Mountain View, CA, USA) equipped with an excitation laser line at 488 nm and Cell Quest software (Becton Dickinson). The DCF (green fluorescence) was collected in a log scale through a 530±20 band pass filter. Monoparametric histograms of the fluorescence distribution were plotted for the estimation of ROS production.

2.3.2. Glutathione content assay

In a first series of experiments, glutathione (GSH) content was evaluated by flow cytometry using *o*-phthaldialdehyde (OPT) as described by Treumer and Valet [24]. Briefly, the OPT method is based on reaction with both glutathione amino and sulphhydryl groups, yielding a cyclic highly fluorescent product. The OPT-GSH fluorescent product appears in the green fluorescence channel. At different times of incubation, 1×10^6 cells were resuspended in 500 µl 10 mM HEPES N[2-hydroxyethyl]piperazine-N'-[2-ethanesulphonic acid]-buffered saline pH 7.4 and OPT was added (final concentration 1 mM of a stock solution 0.1 M in dimethylformamide). After 5 min of incubation at room temperature, the cells were immediately analysed with a FACSCalibur flow cytometer as above. The OPT-GSH (green fluorescence) was collected in a log scale through a 530±20 band pass filter. Monoparametric histograms of the fluorescence distribution were plotted for the estimation of GSH content.

2.3.3. Evaluation of transmembrane potential using double staining with Rhod123 and PI

Mitochondrial transmembrane potential was assessed by flow cytometry uptake of the cationic lipophilic dye Rhodamine 123 (Rhod123) and propidium iodide (PI) using a commercial product according to the method described by Gorczyca et al. [25]. Briefly, at different times of incubation, approximately 5×10^5 cells for each sample were treated with 4 µl of the Rhod123 stock solution (1 µg/ml final concentration) and incubated for 30 min at 37 °C in the dark. The cells were then washed in PBS and resuspended in 200 µl of binding buffer plus 10 µl of the PI stock solution (10 µg/ml final concentration). The cells, kept in ice, were analysed with a FACSCalibur flow cytometer. The Rhod123 (green fluorescence) and the PI (red fluorescence) were both collected in a log scale through a 530±20 and 575±15 nm band pass filter respectively.

2.4. Assay of caspase-9 activity

At different incubation times after CMI/MI exposure, the cells were washed in PBS and resuspended in ice-cold lysis buffer (50 mM HEPES, 1 mM DTT, 0.1 mM EDTA, 10% glycerol, 0.1% CHAPS, pH 7.4 supplemented with 5 mg/ml leupeptin). After centrifugation at 10,000×g at 4 °C, the supernatant was used for the assay of caspase-9 activity. The protein concentration in the lysate was determined by the Bradford assay (26). 25 µg of cell lysate were incubated in 100 µl of assay buffer (50 mM HEPES, 10 mM DTT, 0.1 mM EDTA, 10% glycerol, 0.1% CHAPS pH 7.4, 100 mM NaCl) containing 200 µM Ac-LEHD-pNA in the presence or absence of the caspase-9 inhibitor 0.1 µM Ac-LEHD-CHO. The samples were incubated at 37 °C in a microtiter plate reader for 16 h. The enzyme-catalysed release of p-nitroaniline was monitored at 405 nm. The conversion of the substrate was linear in time and in amount of protein.

2.5. Apoptosis assays

DNA content was analysed using PI, as previously described (12). At least 20,000 events were collected for each sample using Cell Quest software; debris was excluded from the analysis by an appropriate morphological gate of forward scatter vs. side scatter. Fluorescein isothiocyanate (FITC)-labeled AnnexinV (AnnxV) binding and PI uptake were assessed by flow cytometry using a commercial kit (Boehringer Ingelheim Bioproducts, Vienna, Austria) according to the manufacturer's instructions.

2.6. HPLC assays of thiols, disulphides, protein–thiol mixed disulphides

Glutathione, cysteine, cysteinylglycine and homocysteine and corresponding disulphides and protein–thiol mixed disulphides reduced to thiols

with DTT, were analysed with monobromobimane (mBrB) according to Mansoor's et al. method [27], with slight modifications as below.

2.6.1. Analysis of thiols

At different times of incubation, 200 µl of cells resuspended in PBS (containing 1×10^6 cells) were precipitated with 6% (w/v) TCA (final concentration). After centrifugation of the sample (2 min at 10,000×g), the supernatant was neutralized under saturating conditions of solid NaHCO₃ and incubated with 1 mM monobromobimane (mBrB) (final concentration) in the dark at room temperature for 15 min. After centrifugation (2 min at 10,000×g), 90 µl of the supernatant were acidified with 20 µl 37% HCl and injected into the HPLC column.

2.6.2. Analysis of disulphides

200 µl of resuspended cells (containing 1×10^6 cells) were reacted with 50 µl of 10 mM N-ethylmaleimide (NEM) for 5 min. After deproteinization with 6% TCA (final concentration) and centrifugation at 10,000×g for 2 min, the NEM excess of the supernatant was extracted with dichloromethane (0.2 ml sample + 2 ml dichloromethane). 100 µl of the aqueous phase were brought to neutral pH by the addition of solid NaHCO₃ and treated with 0.5 mM DTT (final concentration) at room temperature for 20 min. An excess of mBrB (2 mM final concentration) was then added and the sample processed as above (see thiols).

2.6.3. Analysis of protein–thiol mixed disulphides

The protein pellet of NEM-treated samples was washed twice with 1 ml of 1.5% (w/v) TCA to remove traces of NEM and low molecular weight compounds in the sample. The pellet was then resuspended in 0.2 ml of 1 mM K₃EDTA. After saturation with solid NaHCO₃, 5 µl of 50 mM DTT were added to the resuspension and the sample was maintained under continuous agitation at room temperature for 20 min. The sample was centrifuged at 10,000×g for 2 min and 100 µl of the supernatant were deproteinized with 40 µl of 60% (w/v) TCA. After centrifugation, 100 µl of the supernatant were neutralized with solid NaHCO₃ up to saturation and reacted with 10 µl of 40 mM mBrB. After 15 min incubation at room temperature in the dark, the sample was acidified with HCl as above.

Samples were injected into the HPLC column. Solvent A was 0.25% (v/v) acetic acid, adjusted to pH 3.09 with 1N NaOH, and solvent B was methanol. The elution profile was as follows: 0–8 min, 20% B; 8–15 min, 20–40% B; 15–25 min, 40–100% B. A constant flow rate of 1.0 ml/min was applied. HPLC separation was performed with a Hewlett-Packard 1100 series apparatus, equipped with fluorescence detection (excitation, 380 nm; emission 480 nm). The retention times for cysteine, cysteinylglycine, homocysteine and glutathione were 6.0, 6.7, 10.1 and 12.2, respectively.

Appropriate concentrations of glutathione, cysteine, cysteinylglycine, homocysteine and corresponding disulphides were used to prepare calibration curves in PBS or in PBS+DTT, respectively. The calibration curves were linear from 0.3 µM to 100 µM (3.2 pmol/injection to 1073 pmol/injection). The detection limit was 2 pmol/injection (injection volume 0.02 ml).

2.7. Enzyme activities

Cells collected by centrifugation, washed twice in PBS and resuspended at 5×10^6 cells/ml in 20 mM Tris–HCl with 0.5 mM K₃EDTA pH 7.6, were lysed by three cycles of freezing (–80 °C) and thawing. After centrifugation at 10,000×g for 2 min at 4 °C, the activities of glucose-6-phosphate dehydrogenase (G-6-PDH), glutathione reductase (GR), glutathione transferase (GST) and glutathione peroxidase (GPX) in the supernatants were assayed spectrophotometrically at 37 °C using a JASCO UV-VIS 550 spectrophotometer. G-6-PDH was detected by modification of the methods described by Glock and McLean [28]. Briefly, the sample was added to a cuvette containing 1 mM NADP⁺ and 1 mM G-6-P in 0.1 mM Tris–HCl pH 7.6, and the reaction was followed at 340 nm for 5 min. The reaction rate was calculated in the last 2 min (3 min time lag). GR was assayed by the method of Calberg and Mannervik [29], while GST was assayed by the method of Habig et al. using 1-chloro-2,4-dinitrobenzene as substrate [30]. GPX was assayed by the method of Wendel using cumene hydroperoxide as substrate [31].

Protein concentration was estimated in the supernatant of lysed cells according to the Bradford method [26].

2.8. Statistics

The results are presented as means \pm S.D. from at least three-six independent experiments. Student's *t*-test was used to assess the significance of differences between the treatment and control groups. Moreover, the same test was used in time-course experiments of glutathione to evaluate the significance of the differences between each incubation time and 0 time.

3. Results

CMI/MI induces ROS generation, GSH depletion and changes in $\Delta\psi_m$.

ROS production (Fig. 1), GSH content (Fig. 2) and mitochondrial changes (Fig. 3) were monitored by flow cyto-

metry in the time interval 0–3 h at increasing CMI/MI doses (0.001–0.1%).

3.1. ROS production

The conversion of DCFH-DA to fluorescent DCF by H_2O_2 was used to monitor ROS production. As shown in Fig. 1, all concentrations of CMI/MI caused an increase of intracellular ROS accumulation starting as early as 0 time after treatment. The cell percentage with increased ROS production at the maximum doses was relatively high and remained rather constant within 30 min of monitoring (>60% of cells with high ROS production). Thereafter, a further marked increase of cell percentage with increased ROS generation occurred at 0.05% and 0.1% CMI/MI and remained high until 3 h after treatment. At the intermediate dose (0.01%), ROS production

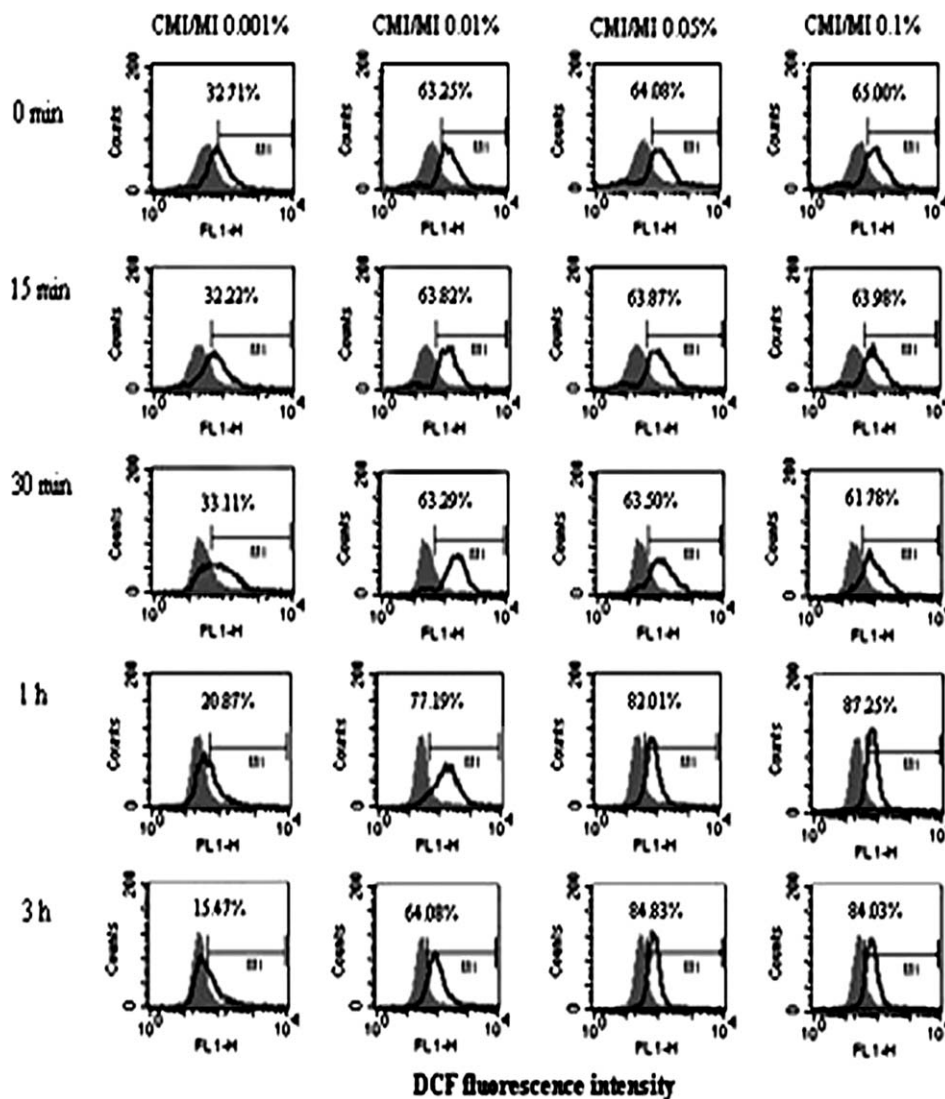


Fig. 1. Flow cytometric analysis of the time-course of ROS generation in HL60 cells exposed to increasing concentrations of CMI/MI. Cells were incubated for 30 min with DCFH-DA, then washed and resuspended in fresh medium and treated with increasing concentrations of CMI/MI (0.001–0.1%) for 10 min, resuspended in fresh medium and incubated at 37 °C. At the indicated times after treatment, the fluorescence intensity was determined by flow cytometry. Similar data were obtained in four independent experiments. Filled histograms correspond to control cells while open histograms represent CMI/MI-treated cells. The x-axis shows log FL-1 fluorescence intensity; the y-axis indicates the cell number. ROS production was quantified as the percentage of cells with increased fluorescence relative to control.

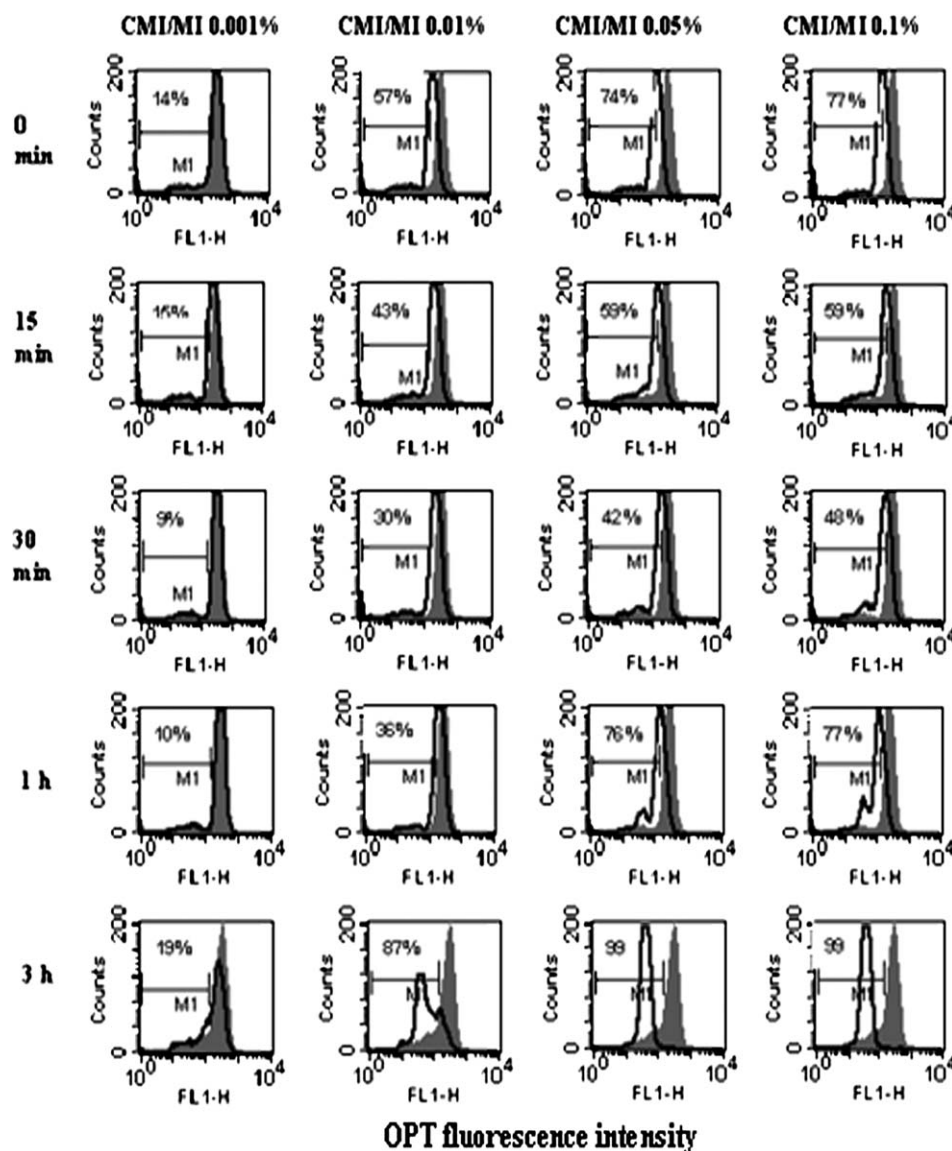


Fig. 2. Flow cytometric analysis of the time-course of GSH content in HL60 cells exposed to increasing concentrations of CMI/MI. Cells were incubated with increasing concentrations of CMI/MI (0.001–0.1%) for 10 min, resuspended in fresh medium and incubated at 37 °C. At the indicated times, untreated and CMI/MI-treated HL60 cells were loaded for 5 min with OPT and the fluorescence intensity was determined by flow cytometry. These experiments were performed three times with very similar results. Filled histograms correspond to control cells, while open histograms represent CMI/MI-treated cells. The x-axis shows log FL-1 fluorescence intensity; the y-axis indicates the cell number. Decreased fluorescence (highlighted by the marker) indicates reduction of GSH content.

remained at medium levels and was nearly constant at all observation times.

At the lowest CMI/MI dose (0.001%), signs of oxidative stress were immediately observed in about 32% of cells. These signs were relatively constant for 30 min, then dropped to about 20% at 1 h and to about 15% by the end of the experiment. Interestingly, there was a clear gap in ROS production between 0.001% and 0.01% CMI/MI at all times.

3.2. GSH changes

We monitored GSH changes in HL60 cells exposed to CMI/MI via the decrease in OPT fluorescence (Fig. 2). CMI/MI treatment at high concentrations (0.01–0.1%) triggered a rapid decrease of intracellular GSH as early as 0 h. GSH levels tended

to recover within 15–30 min, but there was another dramatic GSH decrease between 1 and 3 h. The lowest CMI/MI dose (0.001%) caused a small non-significant decrease in glutathione within 15 min as well as a non-significant GSH recovery over time (9% of depleted cells at 30 min and 10% at 60 min).

To prove the relationship between the extent of GSH depletion and the severity of CMI/MI toxicity, the cells were pre-incubated for 24 h with 500 μ M BSO, which was maintained during the treatment with CMI/MI at different concentrations. Table 1 reports the induction of apoptosis and necrosis in HL60 cells exposed to CMI/MI with and without pre-incubation with BSO.

Cells depleted of GSH (BSO decreased GSH content, as evaluated by monobromobimane, from 55.8 ± 2.3 nmol mg^{-1} proteins to 14.0 ± 2.9 nmol mg^{-1} proteins) were vital and did not

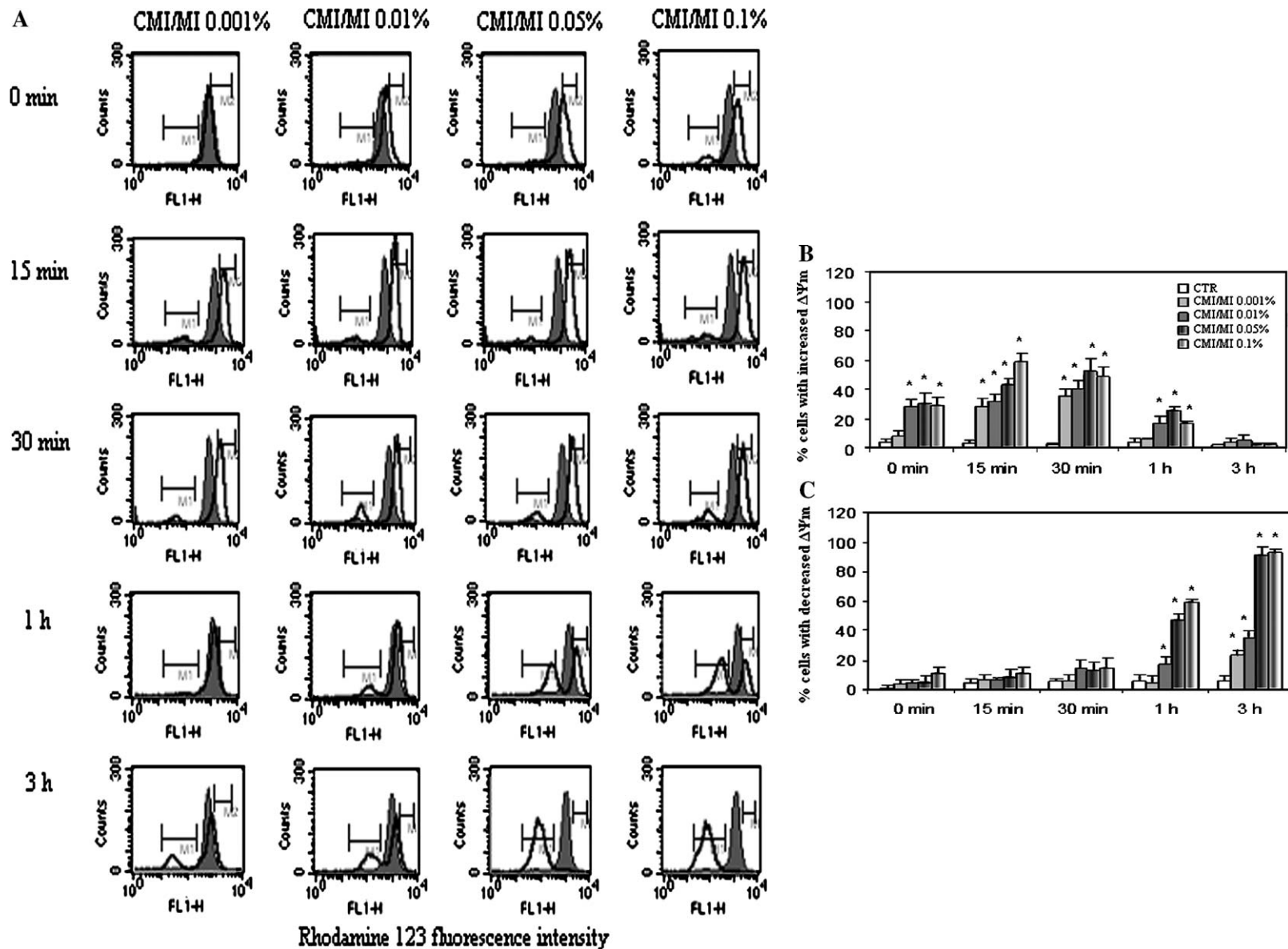


Fig. 3. Flow cytometric analysis of the time-course of mitochondrial transmembrane potential in HL60 cells exposed to increasing concentrations of CMI/MI. At the indicated times, untreated and CMI/MI-treated HL60 cells were loaded for 30 min with Rhod123 and the fluorescence intensity was determined by flow cytometry. (A) Results of a typical experiment where filled histograms correspond to control cells, while open histograms represent CMI/MI-treated cells. The x-axis shows log FL-1 fluorescence intensity; the y-axis indicates the cell number. Increased or decreased fluorescence (highlighted by the markers) indicates increase or reduction of mitochondrial transmembrane potential ($\Delta\psi_m$). Panels B and C report the percentages \pm S.D. ($n=4$) of cells with increased or decreased fluorescence, respectively. *Statistically significant with respect to control $P<0.05$ (Student's t -test).

Table 1
Induction of apoptosis and necrosis in HL60 cells exposed to increasing concentrations of CMI/MI with and without preincubation with BSO

CMI/MI concentration	Apoptosis Sub-G1 (%)				AnnxV-positive and PI-negative cells (%)		AnnxV-positive and PI-positive cells (%)	
	3 h		6 h		3 h		3 h	
	–	+BSO	–	+BSO	–	+BSO	–	+BSO
CTR	0.24	0.50	0.68	0.73	1.3	0.46	1.5	1.46
0.001%	5.48	8.30	9.05	15.06	12.37	20.91	1.54	3.2
0.01%	19.51	1.60	37.71	8.67	8.59	1.04	33.69	79.65
0.05%	1.73	1.05	2.41	1.20	2.15	0.13	94.01	95.20
0.1%	1.23	1.13	1.33	1.01	1.17	0.20	98.56	99.13

Cells were incubated for 24 h with and without BSO 500 μ M and treated with CMI/MI (0.001–0.1%) for 10 min, resuspended in fresh medium and incubated at 37 °C for 3 and 6 h. The induction of apoptosis, evaluated by flow cytometry, is reported as the percentage of cells showing subdiploid DNA content (Sub-G1), the percentage of annexin V (AnnxV)-positive and propidium iodide (PI)-negative cells (early apoptotic cells), and the percentage of AnnxV-positive and PI-positive cells (late apoptotic/necrotic cells). Values are the average of five separate experiments.

go into apoptosis. Cells treated with CMI/MI at apoptotic concentrations exhibited an increase in both the cellular content of subdiploid DNA and externalization of phosphatidylserine (AnnxV-positive and propidium iodide-negative). However, in cells pre-incubated with BSO, both these markers of apoptosis were increased after treatment with 0.001% CMI/MI and were decreased or absent after 0.01% CMI/MI. Moreover, after treatment with BSO and 0.01% CMI/MI, the percentage of AnnxV-positive and PI-positive cells was increased, indicating loss of plasma membrane integrity, as occurred at necrotic doses of CMI/MI.

3.3. $\Delta\psi_m$ changes

We examined changes in $\Delta\psi_m$ in CMI/MI-treated HL60 cells to clarify the role of mitochondria, since mitochondrial functionality is a crucial factor in cytotoxic processes leading to apoptosis. Using Rhod123, a cationic lipophilic dye readily incorporated into mitochondria in a manner dependent on mitochondrial transmembrane potential ($\Delta\psi_m$), we were able to evaluate mitochondrial changes in HL60 cells from 0 to 3 h after CMI/MI treatment.

Untreated cells and cells treated with CMI/MI were loaded with Rhod123. The fluorescence intensity was then analysed by flow cytometry and plotted as a fluorescence histogram. Fig. 3A illustrates the time-course of changes in $\Delta\psi_m$ after CMI/MI treatment. After 10 min of exposure to CMI/MI, a subpopulation of cells gained green fluorescence (consistent with higher $\Delta\psi_m$) as early as 0 time and increased over time until 30 min after treatment at all doses (Fig. 3A and B). Then, the percentage of hyperpolarized cells decreased at 1 h (Fig. 3A and B). At the same time (1 h), about 17%, 49% and 60% of cells, treated respectively with 0.01%, 0.05% and 0.1% CMI/MI, showed significantly decreased $\Delta\psi_m$ with respect to control (Fig. 3A and C). At the lowest CMI/MI dose

(0.001%), the percentage of hyperpolarized cells returned to control levels at 1 h after treatment (Fig. 3A and B), while cells with reduced $\Delta\psi_m$ appeared only after 3 h (Fig. 3A and C). At 0.05% and 0.1% CMI/MI, nearly all cells (95%) showed a loss of $\Delta\psi_m$ at 3 h.

3.4. CMI/MI induces caspase-9 activation and apoptosis

The well-documented disruption of $\Delta\psi_m$ prompted us to evaluate activation by CMI/MI of caspase-9, an apical enzyme in the mitochondrial pathway of apoptosis [32]. We reported previously [9] that a caspase-3-like increase was most evident 3 h after a 10-min exposure to CMI/MI, and that this was the time at which the marker of apoptosis appeared. Therefore, we decided to evaluate caspase-9 (a caspase located upstream of caspase-3 in the caspase signalling cascade) at 1.5 h and 3 h, as these should have been the most appropriate times to record increased caspase-9 activity. In effect, Fig. 4 shows that caspase-9 was activated in a dose-dependent manner at apoptotic doses of CMI/MI (0.001% and 0.01%). In particular, maximal activation was observed at 3 h at 0.01%, whereas no activation was obtained at any time at necrotic doses (0.05% and 0.1%, data not shown). The activation of caspase-9 at apoptotic concentrations was completely blocked by addition of the caspase-9 inhibitor Ac-LEHD-CHO to the mixture (data not shown).

3.5. Changes of thiols and S-glutathionylation of proteins induced by CMI/MI

To confirm the GSH depletion over time seen in Fig. 2 and to better clarify the mechanism of CMI/MI cell metabolism, we studied changes of GSH and other thiols, such as cysteine, homocysteine and cysteinylglycine, and corresponding disulphides and protein–thiol mixed disulphides via HPLC. However, only glutathione and cysteine were detectable in our experimental conditions.

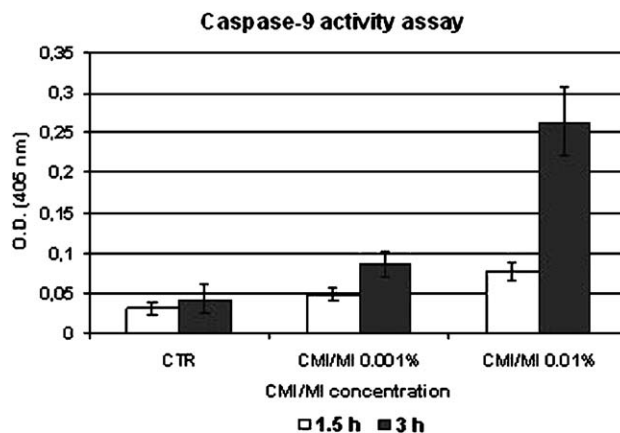


Fig. 4. Time-course of caspase-9 activity in HL60 cells treated with increasing concentrations of CMI/MI. Lysates (25 μ g) made from CMI/MI-treated HL60 cells at different times after treatment were incubated in 100 μ l of assay buffer containing the specific Tetrapeptide substrate, Ac-LEHD-pNA (200 μ M). Caspase activity is expressed as the O.D. 405 nm value \pm S.D. ($n=3$).

3.5.1. Thiols

Dose-related GSH depletion was observed at all times (Fig. 5A), confirming previous results obtained at the cytofluorimeter. After the immediate depletion at 0 h, only 0.001% CMI/MI-treated cells showed a recovery to the control GSH levels at 1 h and 3 h, with a significant increase compared with 0 time, whereas at the other doses (0.01%, 0.05%, 0.1%) the cells did not show a recovery to their control GSH levels even if there was a significant increase (in some cases) with respect to 0 time.

In contrast to the remarkable GSH depletion, cysteine did not change over time (control value: 3.62 ± 1.89 nmol mg⁻¹ proteins; data not shown).

3.5.2. Disulphides and protein–thiol mixed disulphides

There was no significant oxidized glutathione (GSSG) change with respect to control, except at the highest CMI/MI doses (0.05%–0.1%), i.e. at 3 h the levels were significantly decreased with respect to 0 h (Fig. 5B).

The glutathione–protein mixed disulphide (GSSP) data (Fig. 5C) indicated a strong oxidant action by CMI/MI, except at the lowest CMI/MI dose (0.001%). In fact, there was a large gap between 0.001% and the higher CMI/MI doses. In particular, the GSSP increase was very high at 0 time at 0.01%, 0.05% and 0.1% CMI/MI and then decreased significantly at 3 h with respect to 0 h. However, the GSSP decrease over time was higher at 0.01% CMI/MI and the GSSP levels peaked earlier (0 h) than at the other doses.

Cystine and cysteine–protein mixed disulphides (cystine control value: 21.1 ± 7.4 nmol/mg of proteins; cysteine–protein mixed disulphide control value: 1.32 ± 0.84 nmol/mg of proteins; $n=4$) did not vary significantly with respect to control (data not shown).

3.6. The antioxidant response of GSH-related enzymes to CMI/MI

We decided to investigate the role played by various glutathione-dependent enzymes (G-6-PDH, GR, GPX, GST) that have great importance to regulate the intracellular redox state of GSH and whose activity has been related, to some extent, to the presence of available protein SH groups (PSH) [33–35]. Although GPX activity (data not shown) did not change with respect to control, the activities of G-6-PDH, GR and GST decreased in a dose-dependent manner at all times (Fig. 6). The most susceptible enzyme was GR whose activity dropped to about 60% of control at the lowest CMI/MI dose (0.001%) at 0 time.

4. Discussion

Isothiazolinone (or isothiazolone)-derived compounds, such as Kathon CG (a 3:1 mixture of CMI and MI), are used for various purposes as preservatives and biocides [36]. However, Kathon CG may cause occupational diseases such as dermatitis and allergic sensitization [37]. CMI is considered a strong sensitizer, while MI is a weak sensitizer. In spite of these electrophilic differences, evaluated in reactions with amino

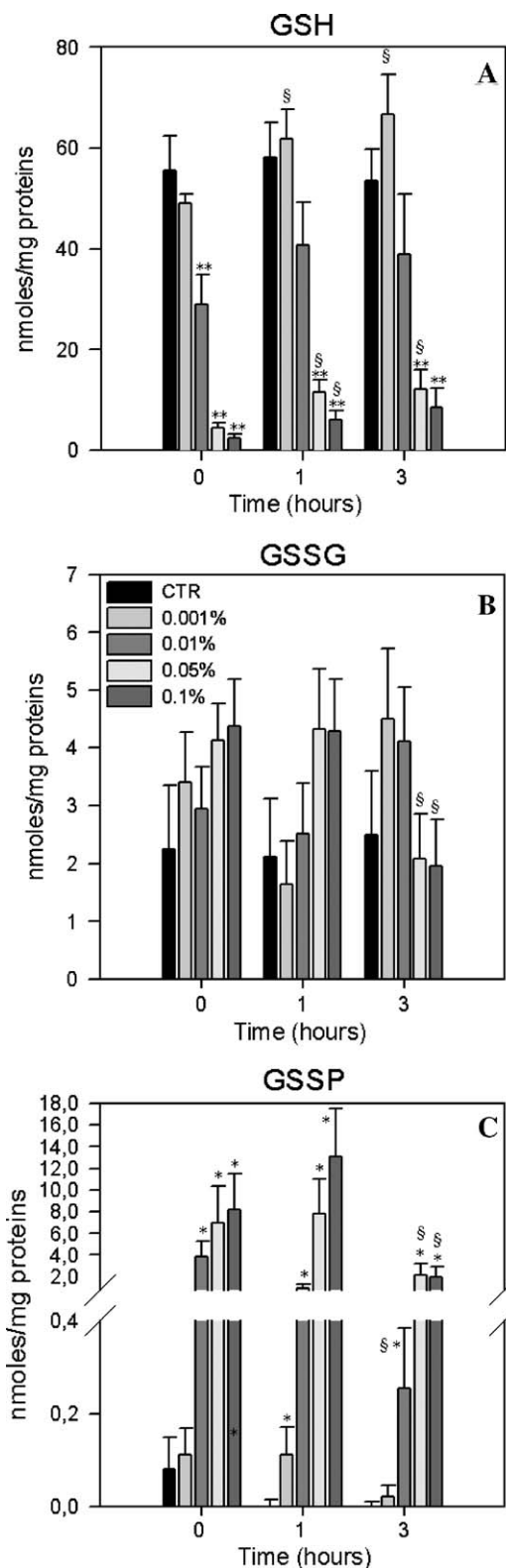


Fig. 5. Time-courses of GSH, GSSG and GSSP in HL60 cells treated with 0.001–0.1% CMI/MI. GSH (A); GSSG (B); GSSP (C) were determined by HPLC after mBrB derivatization (see Materials and methods). The values are expressed as mean \pm S.D. nmol mg⁻¹ proteins ($n=6$). *Statistically significant with respect to control $P<0.05$ (Student's t -test). **Statistically significant with respect to control $P<0.001$ (Student's t -test). §statistically significant with respect to 0 time $P<0.05$ (Student's t -test).

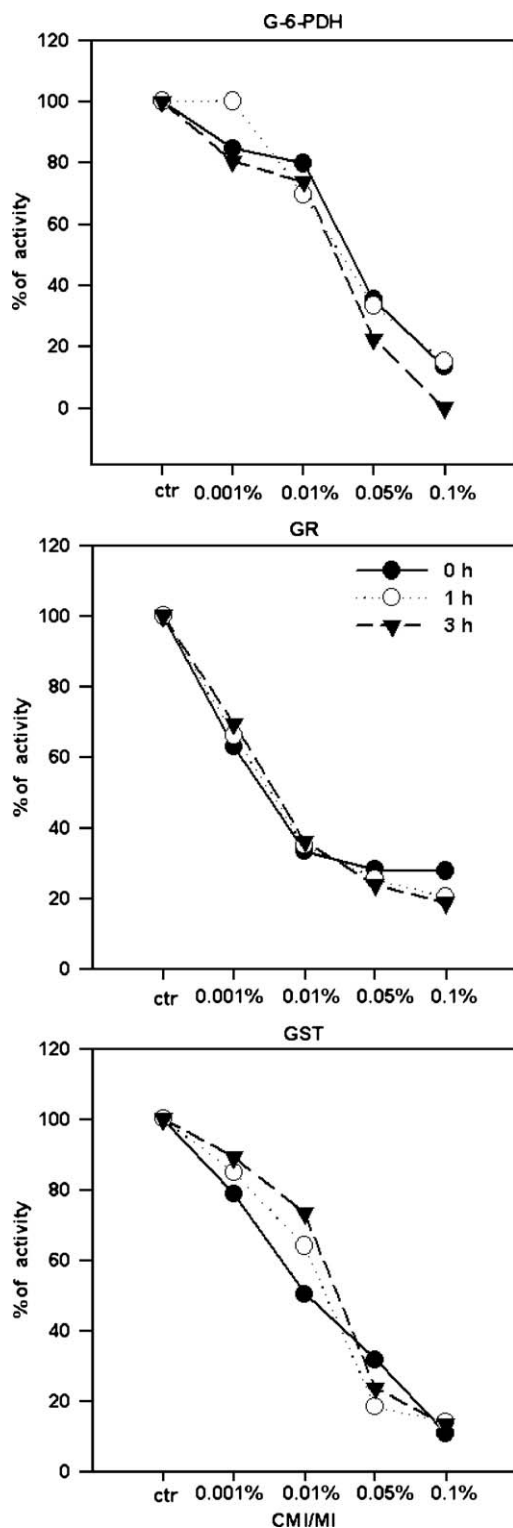


Fig. 6. Activity of G-6-PDH, GR, GST in HL60 cells treated with 0.001%–0.1% CMI/MI. Mean values are expressed as percentage of activity ($\text{nmol min}^{-1} \text{mg}^{-1}$ proteins). The control activities were: G-6-PDH $311 \pm 41 \text{ nmol min}^{-1} \text{mg}^{-1}$ proteins; GR $184 \pm 6 \text{ nmol min}^{-1} \text{mg}^{-1}$ proteins; GST $236 \pm 34 \text{ nmol min}^{-1} \text{mg}^{-1}$ proteins, of three independent experiments whose standard deviation (omitted for clarity) did not exceed 15% of the mean.

groups (histidine and lysine), CMI and MI react much faster with thiols, the most potent nucleophiles [15], and thus can be considered strong GSH depletors in cells. For example, although MI is less reactive than CMI, it can easily attack GSH, as recently demonstrated in cultured neurons [13]. In theory, CMI/MI can also attack exposed PSH, but this action should be prevented by the relatively high GSH concentration in cells.

We reported previously that CMI/MI at low concentrations (0.001% and 0.01%) induced apoptotic death in HL60 cells (as documented by subdiploid DNA content and phosphatidylserine exposure) via caspase-3, while at higher concentrations (0.05% and 0.1%) the response was necrosis [9]. More recently, we reported that CMI/MI also causes apoptosis and oxidative stress in human keratinocytes [12].

The aims of the present experiments on HL60 cells, an appropriate model of apoptosis, were to clarify the mechanism of CMI/MI toxicity towards thiols and to evaluate whether CMI/MI induces GSH depletion by oxidative stress, an event that is considered important for activation of cells to apoptosis and necrosis [19]. The results show that the cytotoxicity of CMI/MI in HL60 cells is associated with ROS generation (Fig. 1), GSH depletion (Fig. 2) and changes in mitochondrial transmembrane potential (Fig. 3). All these biochemical perturbations are much greater during necrosis than during apoptosis. Brief incubation (10 min) of HL60 with CMI/MI was able to trigger a dose-dependent increase in cellular oxidation states as early as 0 min. At the lowest CMI/MI concentration (0.001%), the ROS increase, more pronounced at 0 time, was not accompanied by GSH depletion (Fig. 2). Conversely, at the highest CMI/MI doses, GSH was depleted rather suddenly and this was matched by abundant ROS production, so it was difficult to discern whether the intracellular ROS production preceded the drop in GSH levels or vice versa. Therefore, it is not clear whether the GSH depletion is the cause or the result of ROS generation.

Having re-examined the role of GSH in subsequent experiments to clarify whether the GSH depletion by CMI/MI was due to GSH-conjugation or GSSG formation, we confirmed that there was no GSH depletion at the lowest CMI/MI dose (0.001%) and strong GSH depletion at the higher doses (0.01%, 0.05% and 0.1%) (Fig. 5A). Only a fraction of the GSH lost at all CMI/MI concentrations was converted to GSSG, suggesting that other mechanisms are involved in the GSH depletion. It has been reported that cells undergoing apoptosis exhibit increased GSSG levels [38] or alternatively export GSH into the extracellular space [39]. We evaluated GSH in the cell culture medium at all times after CMI/MI exposure but the GSH level remained constant during the experiments (data not shown), suggesting that the loss of GSH was probably not due to an efflux of GSH. As both CMI and MI were found to react very rapidly with GSH [15], we cannot rule out the possibility that a direct reaction between GSH and CMI/MI occurred in our experimental conditions, with the formation of a GSH-conjugate [15]. This suggestion is confirmed by the fact that total GSH (sum of GSH, GSSG and GSSP) was always lower than the respective control at each time at 0.01%, 0.05% and

0.1% CMI/MI (e.g. total GSH depletion at 0.01% CMI/MI at 0 h, 1 h, 3 h: 36%, 25%, 20%, respectively; total GSH depletion at 0.1% CMI/MI at 0 h, 1 h, 3 h: 60%, 56%, 67%, respectively), but not at the lowest dose (0.001%) where total GSH was equal to or higher than control (data not shown). Therefore, we suggest that part of the GSH was consumed for the formation of GSH-CMI/MI adducts.

It has been reported that a loss of GSH sensitizes cells to the induction of apoptosis, while a loss of GSH is not sufficient itself to initiate apoptosis [21,22,39,40]. We also observed that pre-treatment for 24 h with BSO, a selective inhibitor of gamma-glutamylcysteine synthetase, does not cause apoptosis in HL60 cells despite a marked decrease of cellular glutathione; instead, it clearly switches the mode of cell death from apoptosis to necrosis at 0.01% CMI/MI.

Mitochondria play an essential role in many types of apoptotic death, releasing cytochrome *c*, which triggers a cascade of caspase activation events. Consistent with these observations, CMI/MI caused at all doses an early increase of $\Delta\psi_m$, an event associated with several apoptotic pathways [41–43] while at longer times the mitochondrial transmembrane potential collapsed; simultaneously the activation of caspase-9 occurred only at CMI/MI concentrations (Fig. 4) previously always found to be clearly apoptotic [9]. These results show that alterations of mitochondrial function accompany CMI/MI-induced cytotoxicity, as supported by the MTT assay (which is dependent on mitochondrial redox reactions) [9].

S-glutathionylation, through the formation of a mixed disulphide between a protein SH residue and glutathione, is an antioxidant device that reduces the impact of an oxidative stressor but at the same time modulates protein activity if critical PSH are involved, as for example during cell proliferation, apoptosis and differentiation [44–46]. We observed a dose-dependent increase in GSSP at all times (Fig. 5C), except at the lowest CMI/MI dose (0.001%). Low levels of S-glutathionylation (generally rapidly reversible) appear to be associated with the apoptotic response (see the protein glutathionylation trend at 0.01% CMI/MI in Fig. 5), while high and sustained levels are associated with necrosis.

According to the literature [14,15], the high reactivity of CMI/MI towards thiols may be due to a variety of reaction mechanisms and end-products. We assume that the lipophilic character of CMI/MI causes it to react preferentially with PSH rather than with GSH, opening the ring of the CMI/MI structure and forming a mixed disulphide (CMI/MI–protein). In turn, CMI/MI–protein mixed disulphides would generate GSSP at 0 time by a thiol/disulphide exchange reaction with GSH, delivering CMI/MI-SH derivatives (thioacyl chloride) [15]. However, other more complex mechanisms inside the cells could also yield GSSP as end-products [15].

The low or absent protein glutathionylation in control cells and in those exposed to the lowest CMI/MI concentration was considered indirect evidence that these cells efficiently control their intracellular redox state by GR and G-6-PDH activities [33–35]. Despite this, the enzymatic activities of GR, G-6-PDH and GST were highly sensitive to CMI/MI, being very rapidly depressed after exposure to all CMI/MI doses (Fig. 6),

whereas GPX was unchanged (data not shown) (GPX control value: $552 \pm 53 \text{ nmol min}^{-1} \text{ mg}^{-1} \text{ protein}$; $n=3$). In particular, the inhibition of GR and G-6-PDH, potent regulators of GSSG and GSSP levels [33–35], may explain the high protein S-glutathionylation, which at 0 time increased more than 40 fold with respect to control after 0.01% CMI/MI exposure (Fig. 5). At the lowest CMI/MI concentration (0.001%), these enzymes were depressed (Fig. 6) but still sufficiently active to control the GSSP production. The lack of GPX changes is interpreted as the cell's necessity to eliminate excessive ROS production (H_2O_2).

Cysteine-rich membrane receptors, such as Fas antigen (a member of the tumour necrosis factor receptor family), and caspases can be included in the proteins involved in triggering apoptosis that might be regulated by changes in redox status. We investigated if CMI/MI treatment changes the expression of Fas, which is constitutively expressed by HL60 cells. We failed to detect changes in Fas expression at any time after treatment (data not shown); in contrast, increased Fas expression was detected in human keratinocytes treated with 0.01% CMI/MI [12], suggesting that Fas/FasL-mediated apoptosis plays a role in the widely described allergic contact dermatitis reactions to CMI/MI [47].

Caspases (cysteine proteinases implicated as mediators of apoptosis) contain critical thiol groups and are regulated by changes in redox status [48]. At 0.01% CMI/MI, the maximum activity of caspase-9 and caspase-3 [9] occurred at 3 h when the cells barely showed signs of apoptosis (Table 1) and protein glutathionylation was decreased about 10 fold with respect to the value at 0 time (Fig. 5C). Since GSSG and disulfiram inhibit caspase-3 activity via the formation of protein–thiol mixed disulphides [49], we speculate that phenomena of thiolation/dethiolation of caspases might be associated with their activation. No caspase activity was recorded at higher CMI/MI doses (inducing higher levels of protein glutathionylation), suggesting that inhibition of caspase activity (possibly through S-glutathionylation) prevents the appearance of features typical of apoptosis and that the cells are committed to death by necrosis. Therefore, the possibility of caspase glutathionylation is an important issue that deserves further studies to clarify the relationships with activation of the cell death programme.

The lack of a decrease in cysteine levels after CMI/MI exposure cannot easily be explained; in fact, similar to what was observed for glutathione, cysteine depletion was expected because of the high reactivity of CMI/MI with thiols [14]. Therefore, it is unclear why CMI/MI exposure depleted total GSH but not total cysteine.

The picture that emerges from the study of the relationship between CMI/MI cytotoxicity and thiols is that CMI/MI very rapidly perturbs the normal redox balance and shifts HL60 cells into a state of oxidative stress. Given the high reactivity of CMI/MI, GSH or critical PSH can be attacked, opening the CMI/MI structure by cleavage of the S_γN bond and forming a protein–thiol mixed disulphide (or a mixed disulphide), which in turn generates GSSP by thiol/disulphide exchange reactions. The extent and kinetics of GSH depletion and S-glutathionylation appear to determine whether cells undergo apoptosis or

necrosis. We hypothesize that S-glutathionylation of certain thiol groups accompanied by GSH depletion plays a critical role in the molecular mechanism of CMI/MI.

Acknowledgements

We thank Mr. Leonardo Taurisano for his technical assistance, Dr. Simona Tavarini and Dr. Sandra Nuti for helpful discussions regarding the cytofluorimetric analysis and Dr. Peter Christie for the careful English revision. This research was supported in part by grants from MIUR and the Piano di Ateneo per la Ricerca of the University of Siena.

References

- [1] C. Thompson, Apoptosis in pathogenesis and treatment of disease, *Science* 267 (1995) 1456–1461.
- [2] M.O. Hengartner, The biochemistry of apoptosis, *Nature* 407 (2000) 770–776.
- [3] J.D. Robertson, S. Orrenius, Molecular mechanisms of apoptosis induced by cytotoxic chemicals, *Crit. Rev. Toxicol.* 30 (2000) 609–627.
- [4] G. Majno, I. Joris, Apoptosis, oncosis, and necrosis. An overview of cell death, *Am. J. Pathol.* 146 (1995) 3–15.
- [5] G. Denecker, D. Vercammen, W. Declercq, P. Vandenabeele, Apoptotic and necrotic cell death induced by death domain receptors, *Cell. Mol. Life Sci.* 58 (2001) 356–370.
- [6] A.G. Renehan, C. Booth, C.S. Potten, What is apoptosis, and why is it important? *BMJ* 322 (2001) 1536–1538.
- [7] J.F. Kerr, A.H. Wyllie, A.R. Currie, Apoptosis: a basic biological phenomenon with wide ranging implications in tissue kinetics, *Br. J. Cancer* 26 (1972) 239–257.
- [8] H.M. Ellis, J. Yuan, H.R. Horvitz, Mechanism and functions of cell death, *Annu. Rev. Cell. Biol.* 7 (1991) 663–693.
- [9] C. Anselmi, A. Ettore, M. Andreassi, M. Centini, P. Neri, A. Di Stefano, In vitro induction of apoptosis vs. necrosis by widely used preservatives: 2-phenoxyethanol, a mixture of isothiazolinones, imidazolidinyl urea and 1,2-pentandiol, *Biochem. Pharmacol.* 63 (2002) 437–453.
- [10] J. Chandra, A. Samali, S. Orrenius, Triggering and modulation of apoptosis by oxidative stress, *Free Radic. Biol. Med.* 29 (2000) 323–333.
- [11] M.A. Davis, J.A. Flaws, M. Young, K. Collins, N.H. Colburn, Effect of ceramide on intracellular glutathione determines apoptotic or necrotic cell death of JB6 tumor cells, *Toxicol. Sci.* 53 (2000) 48–55.
- [12] A. Ettore, A. Andreassi, C. Anselmi, P. Neri, L. Andreassi, A. Di Stefano, Involvement of oxidative stress in apoptosis induced by a mixture of isothiazolinones in normal human keratinocytes, *J. Invest. Dermatol.* 121 (2003) 328–336.
- [13] S. Du, B. McLaughlin, S. Pal, E. Aizenman, In vitro neurotoxicity of methylisothiazolinone, a commonly used industrial and household biocide, proceeds via a zinc and extracellular signal-regulated kinase mitogen-activated protein kinase-dependent pathway, *J. Neurosci.* 22 (2002) 7408–7416.
- [14] P.J. Collier, A. Ramsey, R.D. Waigh, K.T. Douglas, P. Austin, P. Gilbert, Chemical reactivity of some isothiazolone biocides, *J. Appl. Bacteriol.* 69 (1990) 578–584.
- [15] R. Alvarez-Sanchez, M. Divkovic, D. Basketter, C. Pease, M. Panico, A. Dell, H. Morris, J.P. Lepoittevin, Effect of glutathione on the covalent binding of the 13C-labeled skin sensitizer 5-chloro-2-methylisothiazol-3-one to human serum albumin: identification of adducts by nuclear magnetic resonance, matrix-assisted laser desorption/ionization mass spectrometry, and nano-electrospray tandem mass spectrometry, *Chem. Res. Toxicol.* 17 (2004) 1280–1288.
- [16] B. Gruvemberg, M. Bruze, Can glutathione-containing emollients inactivate methylchloroisothiazolinone/methylisothiazolinone, *Contact Dermatitis* 38 (1998) 261–265.
- [17] K. Xu, P.J. Thornalley, Involvement of glutathione metabolism in the cytotoxicity of the phenethyl isothiocyanate and its cysteine conjugate to human leukaemia cells in vitro, *Biochem. Pharmacol.* 61 (2001) 165–177.
- [18] M. Merad-Boudia, A. Nicole, D. Santiard-Baron, C. Saille, I.M. Ceballos-Picot, Mitochondria impairment as an early event in the process of apoptosis induced by glutathione depletion in neuronal cells. Relevance to Parkinson's disease, *Biochem. Pharmacol.* 56 (1998) 645–655.
- [19] R.S. Fernandes, T. Cotter, Apoptosis or necrosis: intracellular levels of glutathione influence mode of cell death, *Biochem. Pharmacol.* 48 (1994) 675–681.
- [20] D. Van de Dobbels, S. Nobel, J. Schlegel, I.A. Cotgreave, S. Orrenius, A.J. Slater, Rapid and specific efflux of reduced glutathione during apoptosis induced by anti-Fas/APO-1 antibody, *J. Biol. Chem.* 271 (1996) 15420–15427.
- [21] L. Ghibelli, S. Coppola, C. Fanelli, G. Rotilio, P. Civitareale, A.I. Scovassi, M.R. Ciriolo, Glutathione depletion causes cytochrome c release even in the absence of cell commitment to apoptosis, *FASEB J.* 13 (1999) 2031–2036.
- [22] C. Debbasch, P.J. Pisella, M. De Saint Jean, P. Rat, J.M. Warnet, C. Baudouin, Mitochondrial activity and glutathione injury in apoptosis induced by unpreserved and preserved β -blockers on Chang conjunctival cells, *Investig. Ophthalmol. Vis. Sci.* 42 (2001) 2525–2533.
- [23] F.X. Sureda, C. Gabriel, J. Comas, M. Pallàs, E. Escubedo, J. Camarasa, A. Camins, Evaluation of free radical production, mitochondrial membrane potential and cytoplasmic calcium in mammalian neurons by flow cytometry, *Brain Res. Protoc.* 4 (1999) 280–287.
- [24] J. Treumer, G. Valet, Flow-cytometric determination of glutathione alterations in vital cells by o-phthalaldehyde (OPT) staining, *Exp. Cell Res.* 163 (1986) 518–524.
- [25] W. Gorczyca, M.R. Melamed, Z. Darzynkiewicz, Analysis of apoptosis by flow cytometry, in: M.J. Jaroszeski, R. Heller (Eds.), *Flow Cytometry Protocols, Methods in Molecular Biology*, vol. 91, Humana Press Inc, Totowa, NJ, 1998, pp. 217–238.
- [26] M. Bradford, A rapid and sensitive method for the quantitation of microgram quantities of protein utilizing the principle of protein-dye binding, *Anal. Biochem.* 72 (1976) 248–254.
- [27] M.A. Mansoor, A.M. Svardal, P.M. Ueland, Determination of the in vivo redox status of cysteine, cysteinylglycine, homocysteine, and glutathione in human plasma, *Anal. Biochem.* 200 (1992) 218–229.
- [28] G.E. Glock, P. McLean, Further studies on the properties and assay of glucose-6-phosphate dehydrogenase and 6-phosphogluconate dehydrogenase of rat liver, *Biochem. J.* 55 (1953) 400–408.
- [29] I. Carlberg, B. Mannervik, Glutathione reductase, *Methods Enzymol.* 113 (1985) 484–490.
- [30] W.H. Habig, M.J. Pabst, W.B. Jakoby, Glutathione S-transferases. The first enzymatic step in mercapturic acid formation, *J. Biol. Chem.* 249 (1974) 7130–7139.
- [31] A. Wendel, Glutathione peroxidase, *Methods Enzymol.* 77 (1981) 325–333.
- [32] P. Li, D. Nijhawan, I. Budihardjo, S.M. Srinivasula, M. Ahmad, E.S. Alnemri, X. Wang, Cytochrome c and dATP-dependent formation of APAF-1/caspase-9 complex initiates an apoptotic protease cascade, *Cell* 91 (1997) 479–489.
- [33] S. Frosali, P. Di Simplicio, S. Perrone, D. Di Giuseppe, M. Longini, D. Tanganeli, G. Buonocore, Glutathione recycling and antioxidant enzyme activities in erythrocytes of term and preterm newborns at birth, *Biol. Neonate* 85 (2004) 188–194.
- [34] P. Di Simplicio, F. Franconi, S. Frosali, D. Di Giuseppe, Thiolation and nitrosation of cysteines in biological fluids and cells, *Amino Acids* 25 (2003) 323–339.
- [35] P. Di Simplicio, M.G. Cacace, L. Lusini, F. Giannarini, D. Giustarini, R. Rossi, Role of protein-SH groups in redox homeostasis—The erythrocyte as a model system, *Arch. Biochem. Biophys.* 335 (1998) 145–152.
- [36] A.B. Law, N.J. Moss, E.S. Lashen, C.G. Kathon, A new single-component, broad spectrum preservative system for cosmetics and toiletries, in: J.J. Kabara (Ed.), *Cosmetics and Drug Preservation, Principles and Practice*, Marcel Dekker, New York, 1984, pp. 533–557.
- [37] E.J. Primka, J.S. Taylor, Three cases of contact allergy after chemical burns

- from methylchloroisothiazolinone/methylisothiazolinone: one with concomitant allergy to methyldibromoglutaronitrile/phenoxethanol, *Am. J. Contact Dermat.* 8 (1997) 43–46.
- [38] J.M. Esteve, J. Momo, J. Garcia de la Asuncion, J. Sastre, M. Asensi, J. Boix, J.R. Vina, J. Vina, F.V. Pallardo, Oxidative damage to mitochondrial DNA and glutathione oxidation in apoptosis: studies in vivo and in vitro, *FASEB J.* 13 (1999) 1055–1064.
- [39] L. Ghibelli, C. Fanelli, G. Rotilio, E. Lafavia, S. Coppola, C. Colussi, P. Civitareale, M.R. Ciriolo, Rescue of cells from apoptosis by inhibition of active GSH extrusion, *FASEB J.* (1998) 479–486.
- [40] N. Sato, S. Iwata, K. Nakamura, T. Hori, K. Mori, J. Yodoi, Thiol-mediated redox regulation of apoptosis. Possible roles of cellular thiols other than glutathione in T cell apoptosis, *J. Immunol.* 154 (1995) 3194–3203.
- [41] A. Perl, P. Gergely, G. Nagy, A. Koncz, K. Banki, Mitochondrial hyperpolarization: a checkpoint of T-cell life, death and autoimmunity, *Trends Immunol.* 25 (2004) 360–367.
- [42] K. Banki, E. Hutter, N.J. Gonchoroff, A. Perl, Elevation of mitochondrial transmembrane potential and reactive oxygen intermediate levels are early events and occur independently from activation of caspases in Fas signalling, *J. Immunol.* 162 (1999) 1466–1479.
- [43] P.X. Petit, S.A. Susin, N. Zamzami, B. Mignotte, G. Kroemer, Mitochondria and programmed cell death: back to the future, *FEBS Lett.* 396 (1996) 7–13.
- [44] T. Dandrea, E. Bajak, L. Warnard, I.A. Cotgreave, Protein S-glutathionylation correlates to selective stress gene expression and cytoprotection, *Arch. Biochem. Biophys.* 406 (2002) 241–252.
- [45] Y.W. Know, H. Masutani, H. Nakamura, Y. Ishii, J. Yodoi, Redox regulation of cell growth and cell death, *Biol. Chem.* 384 (2003) 991–996.
- [46] C.A. Chrestensen, D.W. Starke, J.J. Mieyal, Acute cadmium exposure inactivates thioltransferase (Glutaredoxin), inhibits intracellular reduction of protein–glutathionyl-mixed disulfides, and initiates apoptosis, *J. Biol. Chem.* 275 (2000) 26556–26565.
- [47] B.R. Alexander, An assessment of the comparative sensitization potential of some common isothiazolinones, *Contact Dermatitis* 46 (2002) 191–196.
- [48] M.B. Hampton, S. Orrenius, Dual regulation of caspase activity by hydrogen peroxide: implication for apoptosis, *FEBS Lett.* 414 (1997) 552–556.
- [49] C.S.I. Nobel, M. Kimland, D.W. Nicholson, S. Orrenius, A.F.G. Slater, Disulfiram is a potent inhibitor of proteases of the caspase family, *Chem. Res. Toxicol.* 10 (1997) 1319–1324.